ELSEVIER

Intermetallics 9 (2001) 443–449

Intermetallics

www.elsevier.com/locate/intermet

Oxidation behavior of TiAl protected by Si + Nb combined ion implantation

X.Y. Li[a,*], S. Taniguchi[b], Y.-C. Zhu[a], K. Fujita[a], N. Iwamoto[a], Y. Matsunaga[c], K. Nakagawa[c]

[a]Ion Engineering Research Institute Corporation, 2-8-1 Tsuda-yamate, Hirakata, Osaka 573-0128, Japan
[b]Department of Materials Science and Processing, Graduate School of Engineering, Osaka University, 2-1 Yamadaoka, Suita, Osaka 565-0871, Japan
[c]Ishikawajima-Harima Heavy Industry Co., Ltd., 1-15, Toyosu 3-Chome, Koto-Ku, Tokyo 135-8732, Japan

Received 22 December 2000; received in revised form 28 February 2001; accepted 2 March 2001

Abstract

The combined ion implantation of Si + Nb at room temperature and at 1173 K with C contamination was employed to improve the oxidation resistance of a γ-TiAl based alloy [Ti–48Al–1.3Fe–1.1V–0.3B (at%)]. The implantation was conducted with a dose of 3.0×10^{21} ions/m^2 and at an accelerate voltage of 50 kV for each element. The isothermal oxidation behavior of above treated alloys was tested at 1173 K for 349.2 ks in air. The oxide scales formed by short-term and long-term oxidation were characterized by AES, SEM and XRD. It was found that the alloy implanted with Si + Nb at 1173 K with C contamination shows excellent long-term oxidation resistance in comparison to that of the room temperature Si + Nb implanted alloy, although the latter also significantly lowers the oxidation rate of non-implanted alloy. A continuous, compact and thus a protective Al_2O_3 layer was formed in the scale of the alloy implanted with Si + Nb at 1173 K with C contamination after long-term oxidation, and this layer contributed to the best oxidation resistance. It is also indicated that the introduction of Si into Nb modified layer and, in particularly C in conjunction with Nb and Si in the modified layer can further effectively favor the formation of the continuous Al_2O_3 layer in the scale on alloy during high temperature oxidation. © 2001 Elsevier Science Ltd. All rights reserved.

Keywords: A. Titanium aluminides, based on TiAl; B. Oxidation; C. Surface finishing; F. Ion-beam methods

1. Introduction

The γ-TiAl based alloy is regarded as a promising high-temperature structural material because of its low density and good mechanical property at high temperature [1]. The insufficient oxidation resistance above about 1100 K, however, limited its practical application as components for automobile or aircraft engine, which often work at elevated temperatures and in aggressive environment. Therefore, the development of appropriate measures, including alloying addition and surface treatment that can effectively improve the high temperature oxidation resistance of this alloy, attracted intensive attentions in recent years [2–7].

It is well known that ion implantation can be employed as a precise tool to alloy the substrate only in the surface layer with various elements. This method has some remarkable advantages such as not changing the size and bulk property of the parts, no the adherence problem which is often encountered in coating treatment, saving the amount of alloying elements and almost not changing the density of the substrate alloy in comparison with bulk alloying [8]. However, its shallow modified layer often prevents ion implantation from providing sufficient and long-term protective effect. Consequently, it is necessary to overcome this shortcoming of ion implantation for practical application. It is expected that combined implantation with the appropriate combination of elements could optimize the constitution of the implanted region. Thus, this is a potential way to further intensify the modification effect relative to the ordinary single element implantation.

Previous investigation on the oxidation behavior of the TiAl alloy protected by ion implantation indicated that a series of elements such as Nb [9–11], Ta [10], W [10], Si [12,13], Mo [12], Al [10,12], Cl [14], etc. show a positive effect, in particular, Nb and Si are most promising. Our further investigation found that the Nb

* Corresponding author. Tel.: +81-72-859-6651; fax: +81-72-859-6299.

E-mail address: xyli@host.ion-unet.ocn.ne.jp (X.Y. Li).

0966-9795/01/$ - see front matter © 2001 Elsevier Science Ltd. All rights reserved.
PII: S0966-9795(01)00024-3

implantation at 1173 K with C contamination (due to the C evaporation at 1173 K from a carbon-crucible where a sample is mounted) more significantly improves the oxidation resistance than the room temperature Nb implantation without C contamination [15]. Therefore, it is speculated that combined implantation of other elements, such as Si and Nb or Si, Nb and C, could also improve the oxidation resistance of the γ-TiAl based alloy.

In this study, combined implantation of Si + Nb to the alloy Ti–48Al–1.3Fe–1.1V–0.3B (at %) was performed at room temperature and at 1173 K with C contamination. Its influence on the isothermal oxidation behavior of this alloy was tested at 1173 K in air for 349.2 ks. The possible modification mechanism was discussed based on the constitution and structure of the oxide scale.

2. Experimental

The chemical composition of the specimens used in this investigation is Ti–48Al–1.3Fe–1.1V–0.3B (at%). The specimens measuring 15×10×2 in mm were cut from the ingot that was produced by Ar-arc skull melting and was annealed at 1373 K for 86.4 ks in a vacuum for homogenization. The phases of the specimen detected by X-ray diffractometry (XRD) are mainly γ phase and few α_2. The specimen surface was ground with a series of SiC paper of up to 1000# and then polished with alumina powders of 0.3 μm in size. The specimens were finally ultrasonically washed in acetone and ethanol bath, and dried in air before ion implantation.

The combined implantation of Si + Nb at room temperature (hereafter represented as RT Si + Nb) was conducted according to the following procedure; first, Si was implanted with a dose of 3.0×10^{21} ions/m^2 at 50 kV and then Nb was implanted under the same conditions. The only difference between the combined implantation of Si + Nb at 1173 K (hereafter represented as 1173 K Si + Nb) and that at room temperature is that the specimen was heated to 1173 K during the ion implantation in the former case. Because the specimen was mounted in a carbon-crucible, C contaminated the substrate and mixed with the implanted element due to the C evaporation from the crucible at 1173 K. Two large surfaces of 15×10 mm of the specimen were implanted only.

The isothermal oxidation test was performed at 1173 K for 349.2 ks in static laboratory air using a thermobalance that can continuously record the mass gain. At the end of isothermal oxidation experiment, the specimen was furnace cooled.

Auger electron spectroscopy (AES) was used to determine the element distribution in the modified layer and the oxide scale. The surface and cross-section morphology of the scale was observed by the scanning electron microscopy (SEM) at an acceleration voltage of 15 kV. The phases in the oxide scale were identified by X-ray diffractometry (XRD) using Cu-K_α radiation at 40 kV and 30 mA.

3. Results

3.1. Depth profile of the modified layer by AES

Fig. 1(a) and (b) show element distribution in the modified layer of the RT Si + Nb implanted and 1173 K Si + Nb implanted alloy analyzed by AES respectively. A layer rich in Nb and Si appeared in the case of RT Si + Nb implanted alloy, shown in Fig. 1(a), the thickness of this layer is about 60 nm. The maximum Nb concentration is about 40 at.% and it is higher than that of Si of about 30 at.%. For the 1173 K Si + Nb implanted alloy, see Fig. 1(b), Si is almost homogeneously distributed in the analyzed region with the low concentration of about 5 at.%. This is partly due to its diffusion during the subsequent long-time 1173 K Nb implantation of 28.8 ks (8 h) for only one side. The thickness of the Nb-enriched layer was doubled relative to that of RT Si + Nb implanted one, but its peak concentration was lowered to about 30 at.%. In addition, it should be

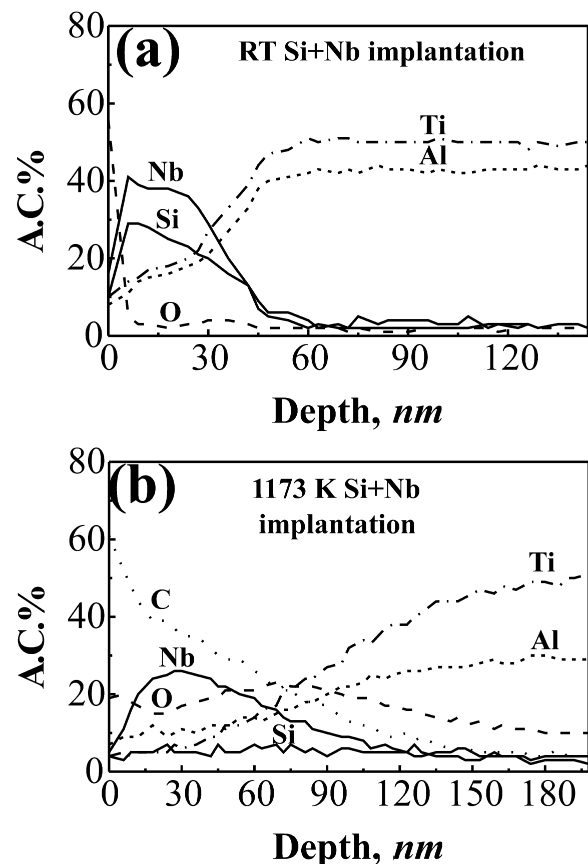

Fig. 1. Depth profile of the modified layer of (a) RT Si + Nb implanted alloy and (b) 1173 K Si + Nb implanted alloy.

noted that a large amount of C was contained in the modified layer. On the surface of the specimen, C shows the higher concentration of about 60 at.%, and it is gradually decreased to about 5 at.% toward the internal region. In the above two cases, Ti composition is always higher than Al, and O was also introduced into the external layer especially for the 1173 K Si + Nb implanted alloy.

3.2. Isothermal oxidation kinetics

Fig. 2 shows the isothermal oxidation curves of RT Si + Nb, 1173K Si + Nb and non-implanted alloy at 1173 K for 349.2 ks in air. For the sake of comparison, the related curves of RT Nb and 1173 K Nb (containing C) implanted alloys are also presented in this figure, and the detail of this work was reported elsewhere [15].

The RT Si + Nb implantation shows better oxidation resistance than the non-implanted and RT Nb implanted alloys. On the other hand, 1173 K Si + Nb (containing C) implantation further remarkably improved the oxidation resistance of the alloy when compared with that of RT Si + Nb and 1173 K Nb (containing C) implanted alloys. Its overall mass gain is the smallest among the above treated alloys and it is only about 1/35 of the non-implanted alloy after oxidation at 1173 K for 349.2 ks. Meanwhile, it is important to note that most mass gain of the 1173 K Si + Nb implanted alloy was obtained in the early stage of the oxidation and it was only increased a little during the following long-term oxidation.

3.3. Characterization of short-term oxidation scale

3.3.1. Oxide scale constitution analyzed by AES

Fig. 3 summarizes the element distribution in the scales of RT Si + Nb and 1173 K Si + Nb implanted alloys after oxidation at 1173 K for 0.9 ks and 10.8 ks analyzed by AES.

After oxidation at 1173 K for 0.9 ks, as shown in Fig. 3(a), the Al enriched layer of about 300 nm thickness was formed in the outer part of the scale of RT Si + Nb implanted alloy. The Nb peak concentration was lowered to about 18 at.%. Si shows homogeneous distribution within the analyzed region and its concentration in the outer part of the scale is about 10 at%. For the 1173 K Si + Nb implanted alloy [Fig. 3(b)], the maximum Nb concentration was reduced to about 18 at.% and it mainly stayed in the scale of about 100 nm depth. The distribution of Si is almost same as that of the as-implanted one [Fig. 1(b)]. A layer rich in Al with a thickness of about 200 nm appeared in the inner part of the scale. It should be noted that C still shows very high content over a 100 nm depth, and O concentration is much smaller in this C rich layer in comparison to that of RT Si + Nb implanted alloy without C contamination [Fig. 3(a)]. Moreover, the oxide scale of 1173 K Si + Nb implanted alloy is much thinner than that of RT Si + Nb implanted alloy after oxidation at 1173 K for 0.9 ks.

When the exposure time was extended to 10.8 ks, as indicated in Fig. 3(c) and (d), an Al enriched layers still existed in their scales, however, it is thicker in the case of 1173 K Si + Nb implanted alloy than that of RT Si + Nb implanted one. For RT Si + Nb implanted alloy [Fig. 3(c)], Ti is much higher than that of Al beneath this Al enriched layer. The Nb and Si show almost similar distribution with the less concentration of about 7 at.% in the scale. On the contrary, for the 1173 K Si + Nb implanted alloy [Fig. 3(d)], it can be found that Ti is just slightly higher than Al below this Al enriched layer, and Al is higher than Ti again toward the internal scale. The C concentration was lowered to about 20 at.% and O shows relatively lower concentration in the outer surface of the specimen. Although Nb and Si are also homogeneously distributed, Nb still shows a small peak concentration in the external scale.

3.3.2. Surface morphology of oxide scale

The surface morphology of the oxide scale after oxidation at 1173 K for 10.8 ks of RT Si + Nb and 1173 K Si + Nb implanted (containing C) alloy is presented in Fig. 4(a) and (b) respectively.

For the RT Si + Nb implanted alloy, as shown in Fig. 4(a), a considerable amount of large particles together with acicular oxide and small-sized oxide grains appeared on the specimen surface. It is believed that the large oxide particles are TiO_2 and the small oxide grains are Al_2O_3 by considering their respective growing rate in this early stage of oxidation, because the TiO_2 grows much faster than Al_2O_3.

The oxide morphology formed on the 1173 K Si + Nb implanted alloy is quite different from that of RT Si + Nb implanted alloy. The uniform and small oxide grains covered the specimen surface [Fig. 4(b)]. Referring to scale composition obtained by AES analysis [Fig. 3(d)], it can be assumed that this oxide is mainly Al_2O_3.

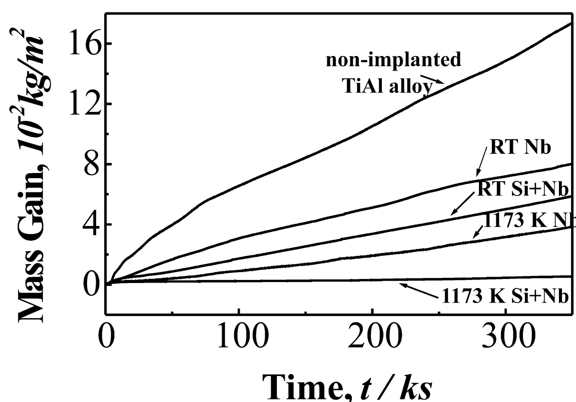

Fig. 2. Isothermal oxidation kinetics at 1173 K for 349.2 ks in air for differently implanted alloys.

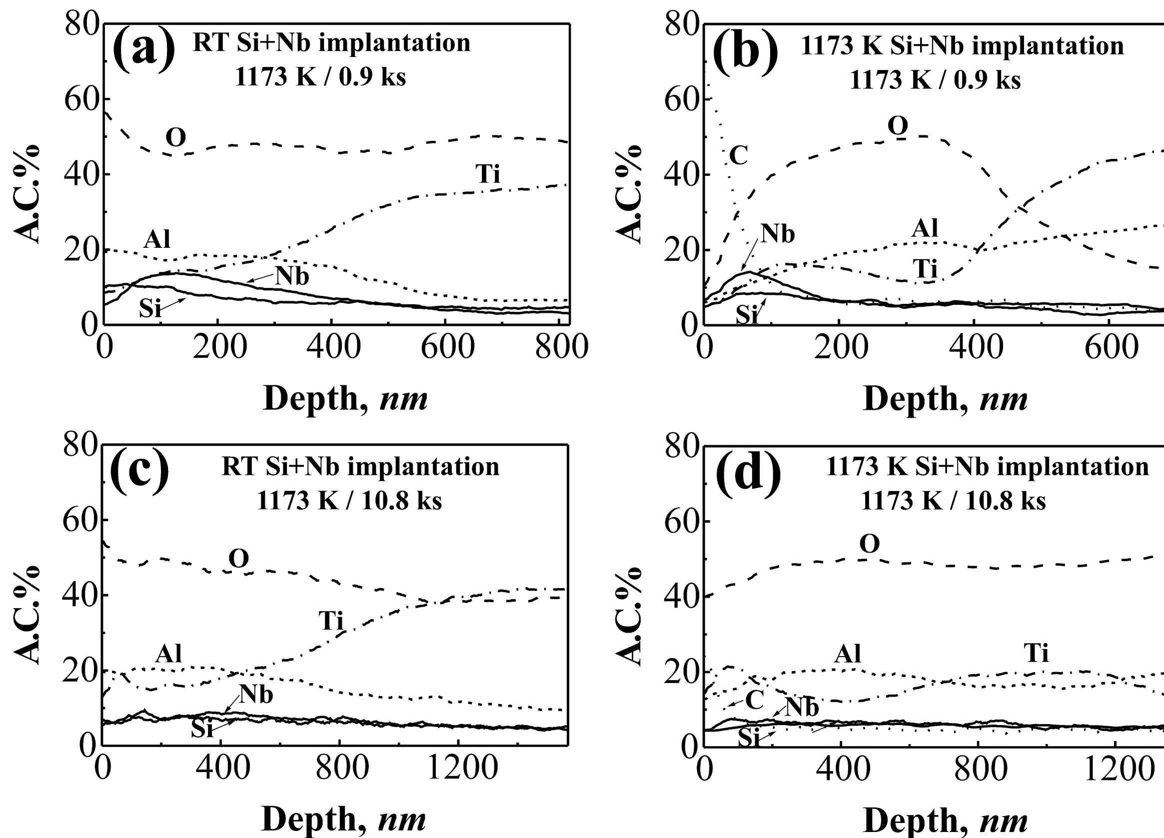

Fig. 3. Depth profile of the scale formed on RT Si + Nb and 1173 K Si + Nb implanted alloy after short-term oxidation.

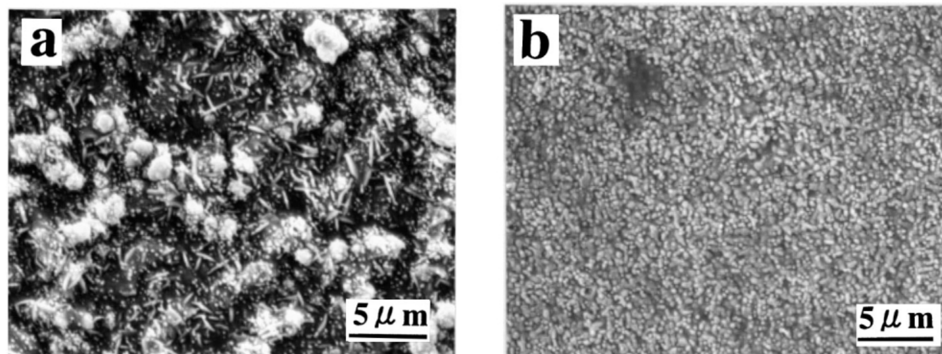

Fig. 4. Surface morphology of (a) RT Si + Nb and (b) 1173 K Si + Nb implanted alloy after oxidation at 1173 K for 10.8 ks in air.

3.4. Characterization of long-term oxidation scale

3.4.1. Surface and cross-section morphology

Fig. 5 shows the surface morphology of non-implanted alloy, RT Si + Nb and 1173 K Si + Nb implanted alloys and its cross-section morphology after oxidation at 1173 K for 349.2 ks in air.

After this long-term oxidation, the oxide on the non-implanted alloy shows the largest grain size [Fig. 5(a)] which consisted mostly of TiO_2. For the RT Si + Nb implanted alloy, the shape of the oxide grain looks like that of the non-implanted alloy but its size became a little small [Fig. 5(b)]. The oxide formed on the surface of 1173 K Si + Nb implanted alloy changed a lot in comparison to the above two cases [Fig. 5(c)]. Its oxide grain is still uniform, compact and small-sized. Concerning its oxide morphology in the early stage of oxidation for 10.8 ks [Fig. 4(b)], it can be assumed that the character of the oxide almost remains unchanged, and the only difference is that its oxide grain size was increased a little.

The oxide scale of 1173 K Si + Nb implanted alloy after oxidation at 1173 K for 349.2 ks in air, Fig. 5(d), consisted of a very thin and continuous oxide layer of

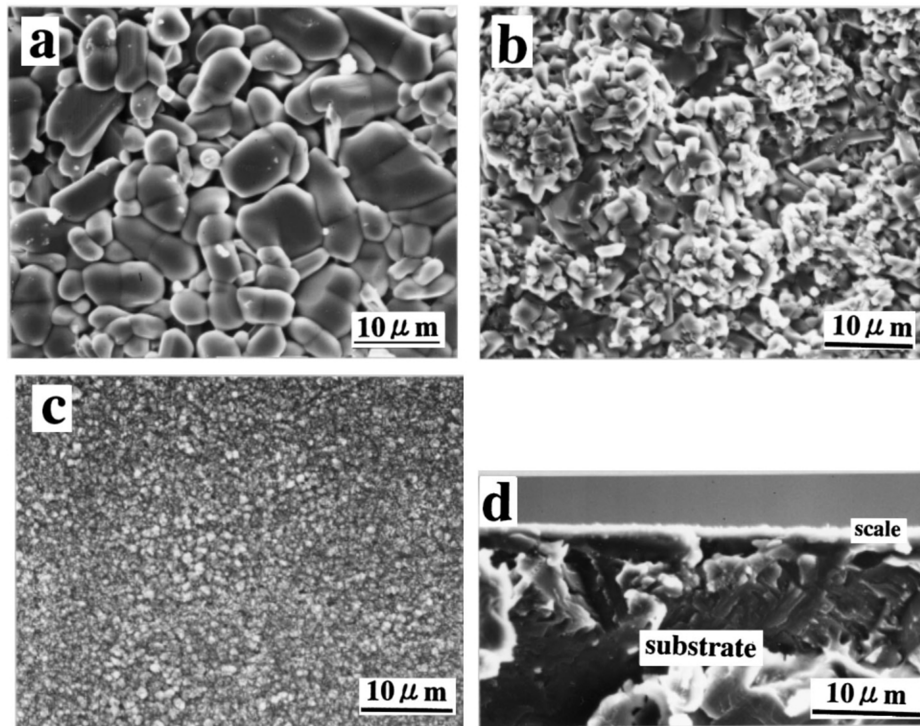

Fig. 5. Surface morphology of (a) non-implanted alloy; (b) RT Si + Nb implanted alloy; (c) 1173 K Si + Nb implanted alloy and (d) cross-section morphology of 1173 K Si + Nb implanted alloy after oxidation at 1173 K for 349.2 ks in air.

about 1 μm thickness. This scale is dense and well adhered with the substrate. Regarding to its surface morphology [Fig. 5(c)] and its overall oxidation kinetics (Fig. 2), it can be concluded that these results are in good agreement and they all reflected that the 1173 K Si + Nb implanted alloy shows the best oxidation resistance among the above differently treated alloys.

3.4.2. Oxide scale composition and phase constitution

The element distribution in the external part of the scale of 1173 K Si + Nb implanted alloy after oxidation at 1173 K for 349.2 ks in air analyzed by AES is presented in Fig. 6. Apparently, the scale essentially consisted of the Al enriched layer with the thickness more than 700 nm after this long-term oxidation, although the Ti concentration is a little high over 100 nm depth. Nb and Si were homogeneously distributed with the concentration of about 5 at.% through the analyzed region. C still shows high concentration of about 20 at.% in the scale surface.

Fig. 7 gives the XRD spectra of the above oxide scale. γ and α_2, which are the main phases of the substrate alloy, show the strongest peaks indicating that a very thin scale was formed even after this long-term oxidation at 1173 K. This has also been proved by its cross-section in Fig. 5(d). For the oxide phases, α- Al_2O_3 shows the highest intensity together with the relatively weak TiO_2 (rutile) peak. This kind of oxide phase constitution was also well coincided with the scale composition obtained by AES analysis (Fig. 6).

By connecting the above AES, XRD results with the surface and cross-section morphology of this scale, it can be concluded that a thin, dense and protective α-Al_2O_3 dominated scale was formed on the 1173 K Si + Nb implanted alloy after oxidation at 1173 K for 349.2 ks.

4. Discussion

Fig. 2 clearly shows that 1173 K Si + Nb implanted alloy exhibited excellent oxidation resistance at 1173 K even for up to 349.2 ks in air. In connection with its oxide scale constitution and structure obtained by AES, SEM and XRD analysis, it is assumed that the formation of a thin, continuous and dense Al_2O_3 scale is responsible for the significant improvement of the oxidation resistance.

The scale structure and oxidation mechanism of the binary TiAl alloy have been intensively investigated [16,17]. It has been proved that, when Al content is less than 50 at.%, an outer Ti oxide layer was preferentially formed and Al_2O_3 only can appear as internal precipitates. One reason is that TiO is more stable than Al_2O_3 and the kinetics of Ti oxide formation is greater than that of Al_2O_3 formation. On the other hand, O shows high permeability in TiAl alloys and Al diffusivity is low in the lower Al containing phases such as Ti_3Al. Al_2O_3 formation only can be favored when the depletion of Ti leads to the Al enrichment below the outer TiO_2 layer.

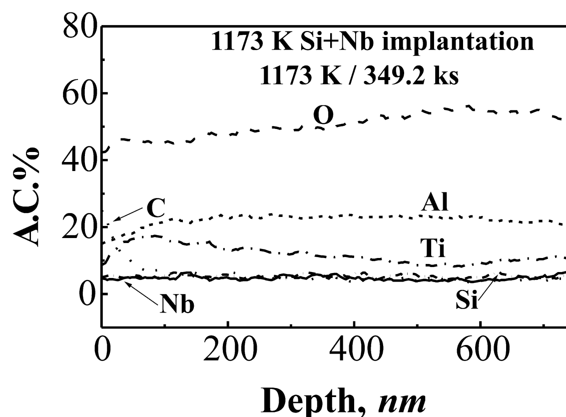

Fig. 6. External scale of 1173 K Si + Nb implanted alloy after oxidation at 1173 K for 349.2 ks in air.

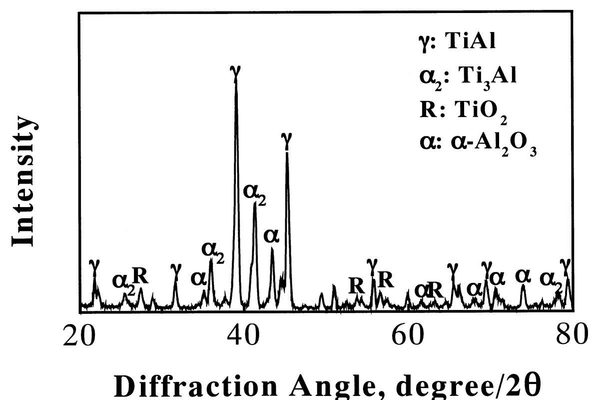

Fig. 7. XRD spectra of the oxide scale of 1173 K Si + Nb implanted alloy after oxidation at 1173 K for 349.2 ks in air.

In addition, the Kirkendall diffusion of Ti leaves large amounts of vacancy in the substrate and this makes the scale become porous. Ultimately, besides the outermost TiO_2 layer, a loose inner oxide layer mixed by TiO_2 and Al_2O_3 was formed after long-term oxidation. This kind of scale readily spalls off from the substrate and can not act as an obstacle to inhibit the further oxidation.

However, as indicated by our results, the oxidation behavior of 1173 K Si + Nb implanted alloy is quite different from non-protected binary TiAl alloy. In the beginning of the oxidation, as proved by Fig. 3(b) and (d) and Fig. 4(b), the Al_2O_3 was preferentially formed. This corresponds to the most mass gain during the early stage of exposure as indicated by its oxidation kinetics curves. Moreover, it should be noted that the beneficial effect which favored the formation of Al_2O_3 resulting from the 1173 K Si + Nb implantation was always maintained during the following long-term oxidation, until a continuous Al_2O_3 layer was formed. After the formation of this protective layer, its oxidation rate becomes much smaller since Al_2O_3 scale exhibits low diffusivities for both the cations and anions as well as being highly stable. Therefore, this alloy eventually shows remarkably low overall mass gain and excellent oxidation resistance for the long-term.

It is important to note that the usual formation of internal precipitates of Al_2O_3 for the non-protected binary alloy was transformed to the formation of a continuous external Al_2O_3 layer by the 1173 K Si + Nb implantation. Considering the critical concentration N* for the transition from internal to external oxidation submitted by Wagner [18], it can be concluded that the Al concentration required for the external scale formation increases with an increase in the solubility and diffusivity of oxygen and decreases with increasing Al diffusivity in the alloy. Thus, the formation of the external Al_2O_3 scale in the case of the 1173 K Si + Nb implanted alloy is essentially due to the change of the above factors caused by the addition of Si, Nb and C elements. Our previous investigation demonstrated that respective RT Si or Nb implantation could improve the oxidation resistance of the TiAl alloy. Their modification mechanisms were intensively studied by several research groups [9–13]. In the case of Nb implantation, the possible reason is that the high surface concentration of Nb could facilitate the formation of β phase in which the diffusion of Al is much faster than in the γ-TiAl phase. In addition, the solubility of O in the substrate could be lowered by the presence of the Nb rich layer [9]. Taking into account the valence-control rule, addition of elements such as Nb which forms cations with a valence bigger than +4 will substitute the Ti and Al ion site in the TiO_2 and Al_2O_3 space lattices and thus reduce the number of metal ion interstital and oxygen vacancies in the oxides [10]. The above effects brought by the Nb implantation contribute to the formation of the Al_2O_3 enriched layer in the external part of the scale during the early stage of oxidation. Furthermore, the mixture of Nb oxide with TiO_2 and Al_2O_3 could improve the adherence of the oxide scale with the substrate [11], this is also beneficial to the long-term oxidation resistance. The effect of Si implantation and the formation of the possible intermetallic phase are significant and sufficient to maintain the Al_2O_3 rich scale [12]. The incorporation of the Si oxide and its form in the early stage scale needs further confirmation. However, the above beneficial effect for respective Nb and Si implantation would gradually be lost, because of the rapid consumption due to the shallow modified layer, before a continuous Al_2O_3 layer was formed in the scale. Consequently, ordinary Nb or Si implantation cannot provide sufficient oxidation resistance for long-term oxidation.

The addition of Si into the Nb modified layer by the RT Si + Nb combined implantation will introduce the above beneficial effect of Si besides the role of Nb and hence the oxidation resistance of single Nb implanted alloy was further improved to some degree.

In the case of the 1173 K Si + Nb implanted alloy, in addition to the presence of Nb and Si, a large amount of

C was introduced into the modified layer. The C enriched layer would effectively lower the concentration of O and prevent its inward diffusion as indicated in Fig. 3(b) and (d). Furthermore, the Nb-loss from the originally implanted layer during the early stage oxidation can also be suppressed by its co-existence with the C rich layer by comparison of Fig. 3(a) and (b) as well as Fig. 3(c) and (d). Thus, the beneficial effect of Nb may be prolonged by the co-existence of Nb and C during the long-term high temperature oxidation. The detailed works of the influence of C and C+Nb co-existence on the oxidation behavior of the TiAl alloy will be shown elsewhere and this can give a good understanding of the C effect [19]. In general, the interaction and the further enhancement of the modified effect of Nb, Si and C eventually resulted in the formation of the continuous Al_2O_3 layer in the scale and the excellent long-term oxidation resistance of the 1173 K Si+Nb implanted alloy. The above discussions of the respective effect of additions of Nb, Si and C are only based on the currently obtained experimental results and related references. It should be pointed out that the comprehensive effect of the co-existence of Nb, Si and C including the possible new phase formation in the as-implanted state or during the early stage of oxidation need further investigation by some advanced analysis tools since the modified layer and initial oxidation scale are very thin.

On the basis of the above results, it should be noted that two factors are worth considering when ion implantation is employed as a surface protective measure to provide long-term oxidation resistance for the TiAl alloy. First, the appropriate combination of elements in the modified layer is required. This can be achieved by suitable implantation process. Secondly, whether the beneficial effect from the modified layer can be maintained long enough to form a continuous and dense Al_2O_3 scale is very important. As revealed by the oxidation kinetics in Fig. 2, the beneficial effect of different implantation is enhanced according to the following sequence: RT Nb, RT Si+Nb, 1173 K Nb (containing C) and 1173 K Si+Nb (containing C). Obviously, it suggests that combined ion implantation by appropriate elements is a possible way to further enhance the modified effect of ordinary implantation with a single element. In the case of the 1173 K Si+Nb (containing C) implanted alloy, the comprehensive beneficial effect of Si, Nb and C is strong enough to form a continuous and protective Al_2O_3 scale and thus offers excellent oxidation resistance at 1173 K for long-term oxidation.

5. Conclusions

(1) The 1173 K Si+Nb (containing C) implanted TiAl alloy shows excellent oxidation resistance at 1173 K at least for 349.2 ks in air relative to RT Si+Nb implanted alloy, although the latter one also significantly decreased the oxidation rate in comparison to that of the non-protected TiAl alloy.

(2) The improvement of the oxidation resistance by 1173 K Si+Nb (containing C) implantation is attributed to the formation of a continuous, compact and protective Al_2O_3 layer in the scale.

(3) The introduction of C into the Si+Nb modified layer during 1173 K Si+Nb implantation could further enhance the beneficial effect Nb and inhibit the inward diffusion of O during oxidation and eventually promote the formation of the continuous Al_2O_3 layer.

Acknowledgements

This work was financially supported by New Energy and Industrial Technology Development Organization (NEDO), MITI, Japan. The authors are also grateful to Mr. J. Nakata for his partial experimental assistance at Osaka University.

References

[1] Kim Y-W. JOM, 411989:24–30
[2] McKee DW, Huang SC. Corrosion Science 1992;33(12):1899–914.
[3] Shida Y, Anada H. Corrosion Science 1993;35(5–8):945–53.
[4] Taniguchi S, Juso H, Shibata T. Oxidation of Metals 1998;49(3/4):325–48.
[5] Kim S, Lee D, Kim I. Mater Sci Technol, May 1999;15:575–82.
[6] Retallick WB, Brady MP, Humphrey DL. Intermetallics 1998;6:335–7.
[7] Taniguchi S, Shibita T, Murakami A. Oxidation of Metals 1994;41(1/2):103–13.
[8] Treglio JR, Perry AJ, Stinner RJ. Advanced Mater and Processes 1995;5:29–32.
[9] Taniguchi S, Shibata T, Saeki T, Zhang H, Liu X. Mater Trans JIM 1996;37(5):998–1003.
[10] Zhang YG, Li XY, Chen CQ, Zhang TH, Zhang XJ, Zhang HX. In: Nathal MV, Darolia R, Liu CT, Martin PL, Miracle DB, Wagner R, Yamaguchi M, editors. Structural intermetallics, The Minerals, Metals and Materials Society, 1997, p. 353–60.
[11] Stroosnijder MF, Zheng N, Quadakkers WJ, Hofman R, Gil A, Lanza F. Oxidation of Metals 1996;46(1/2):19–35.
[12] Taniguchi S, Uesaki K, Zhu Y-C, Matsumoto Y, Shibita T. Mater Sci Eng 1999;A266:267–75.
[13] Taniguchi S, Kuwayama T, Zhu Y-C, Matsumoto Y, Shibita T. Mater Sci Eng 2000;A277:229–36.
[14] Schumacher G, Dettenwanger F, Schutze M, Hornauer U, Richter E, Wieser E, Moller W. Intermetallics, 71999:1113–20
[15] Li XY, Zhu Y-C, Fujita K, Iwamoto N, Matsunaga Y, Nakagawa K, Taniguchi S. Mater Trans JIM 2000;41(9):1157–60.
[16] Taniguchi S, Shibata T, Itoh S. Mater Trans JIM 1991;32(2):151–6.
[17] Shida Y, Anada H. Mater Trans JIM 1993;34(3):236–42.
[18] Wagner C. Z Elektrochem 1959;63:772–82.
[19] Li XY, Taniguchi S, Zhu Y-C, Fujita K, Iwamoto N, Matsunaga Y. et al. Mater. Sci. Eng. (A) (in press).